EVALUATION OF NANOFLUIDS PERFORMANCE FOR SIMULATED MICROPROCESSOR

Aysha Maryam SIDDIQUI[1], Waqas ARSHAD[2], Hafiz Muhammad ALI[2]*, Muzaffar ALI[2] and Muhammad Ali NASIR[2]

[1]Department of Electrical Engineering, COMSATS Institute of Information Technology, Wah, Pakistan

[2]Department of Mechanical Engineering, University of Engineering and Technology, Taxila, Pakistan

* h.m.ali@uettaxila.edu.pk

In this investigation, deionized water was used as base fluid. Two different types of nanoparticles, namely Aluminium oxide and Copper were used with 0.251% and 0.11% volumetric concentrations in the base fluid respectively. Nanofluids cooling rate for flat heat sink used to cool a microprocessor was observed and compared with the cooling rate of pure water. An equivalent microprocessor heat generator i.e. a heated copper cylinder was used for controlled experimentation. Two surface heaters, each of 130 W power, were responsible for heat generation. The experiment was performed at the flow rates of 0.45 LPM, 0.55 LPM, 0.65 LPM, 0.75 LPM and 0.85 LPM. The main focus of this research was to minimize the base temperature and to increase the overall heat transfer coefficient. The lowest base temperature achieved was 79.45 ^{o}C by Aluminium oxide nanofluid at Reynolds number of 751. Although, Al_2O_3/H_2O nanofluid showed superior performance in overall heat transfer coefficient enhancement and thermal resistance reduction as compared to other tested fluids. However, with the increase of Reynolds number, Cu/H_2O nanofluid showed better trends of thermal enhancement than Al_2O_3/H_2O nanofluid, particularly at high Reynolds number ranges.

Keywords: *nanofluid, specific heat, thermal capacity, enhancement*

Introduction

In computer industry, as processor's performance is being improved, cooling system's performance becomes a big technical challenge. On the other hand, size of computer is being reduced rapidly. So, there is a need to improve the cooling techniques to maintain the temperature in safe threshold range because conventional air cooling technique has reached its maximum limit in heat removing capacity. Nowadays, research in the field of heat transfer by liquid has attracted increasing interest due to higher thermal capacity of liquid. Research on this subject can be divided into two parts. The first one is

* h.m.ali@uettaxila.edu.pk

modification of heat sink geometry with ordinary fluid and second one is modification of thermo physical properties of fluids with simple geometry in order to maintain proper functioning of electronic products.

About thirty years ago, Tuckerman and Pease [1] reported a study on the microchannel heat sinks. They showed that by decreasing channel's hydraulic diameter, higher heat transfer could be achieved. This perspective gave new idea for research. Subsequently, the concept of heat transfer improvement by decreasing channel's hydraulic diameter up to micro level has been adopted for other application [2-4].

Xie *et al.* [5] performed a numerical study on minichannel with water as a coolant and concluded that the heat transfer increased by decreasing channel width, bottom thickness of channel and by increasing channel depth. They found optimized configuration of heat sink, which was capable to remove heat up to 256 W/cm^2 by only 0.205 W pumping power, which was much higher than the maximum heat removed by air i.e. 100 W/cm^2.

Steinke and Kandlikar [6] studied different enhancement techniques that can be implemented on microchannels. Those included different techniques like entrance effects, flow obstruction, secondary flows, curved path of flow, surface roughness increment and addition of solid particles in coolants. The dynamic techniques included coolant or surface vibration, varying flow rate, exposed flow to electric field.

Nowadays, novel cooling techniques are required to improve the cooling efficiency of computer processor. Thus, researchers focused on cooling by special kind of fluid having high conductive 'nano' particles. Water based nanofluids with various nanoparticles offer better cooling mechanism [7-9]. These fluids have better thermal properties. Convective heat transfer performance investigated experimentally by many researchers using different concentrations of Al_2O_3 nanofluids [10].

Sohel *et al.* [11] examined Al_2O_3/H_2O nanofluid with four different volumetric concentrations (0.1%, 0.15%, 0.20%, and 0.25%) and compared those results with distilled water. They found that thermal effectiveness was increased up to a certain limit of flow rate, after that a decrease in thermal effectiveness was occurred. Higher concentration of nanofluids always showed better thermal effectiveness for all flow rates. They found 18% heat transfer coefficient enhancement compared to water by 0.25% vol. concentration.

Ho *et al.* [12] assessed forced convection heat transfer of Al_2O_3/H_2O nanofluid with two volumetric concentrations (1% and 2%) and compared results with water. They observed 2% vol. nanofluid was less efficient than that of 1% vol. nanofluid due to less variation occurrence in dynamic viscosity with temperature. They found 70% enhancement in convective heat transfer coefficient compared to water using 1% vol. concentrated alumina nanaofluid.

Generally heat transfer rate increases with the increase of flow rate. However, this is not always true especially for the higher flow rates. Anoop *et al.* [13] used three concentrations of water based SiO_2 nanofluids to find heat transfer rate flowing through microchannel fabricated by Poly Di-Methyl Siloxane in Reynolds number range of 4-22. All three weight concentrations (0.2%, 0.5%, 1%) of SiO_2/H_2O nanofluids showed better heat transfer enhancement at lower Reynolds number as compared to heat transfer enhancement at higher Reynolds number with respect to water.

Rafati *et al.* [14] used ethylene glycol and deionized water based nanofluids having three different volumetric concentrations of alumina, silica and titania. They performed test at three different

flow rates of 0.5 LPM, 0.75 LPM and 1.0 LPM and showed prominent reduction of base temperature by increasing flow rate. 1.0% concentrated alumina nanofluid showed better performance and reduced base temperature by 5.5 °C compared to base fluid.

Dixit and Ghosh [15] experimentation involved straight, diamond and offset minichannels. They found that Nusselt number varied linearly with Reynolds number, and remained invariant to heat flux. They also observed that thermal resistance was inversely proportional to fluid flow rate. A higher pressure drop was observed in diamond minichannel as compared to offset minichannel.

Peyghambarzadeh *et al.* [16] reported experimental investigation on water based CuO and Al_2O_3 nanofluids with 0.2% and 1% volumetric concentration respectively. CuO nanofluid showed better performance as compared to Al_2O_3 nanofluid. Heat transfer coefficient enhancement was up to 27% and 49% with CuO and Al_2O_3 nanofluid respectively.

Corcione [17] gave empirical correlation for the dynamic viscosity and thermal conductivity of nanofluids based on available experimental data. He found that the ratio of nanofluid and base fluid thermal conductivity increased by decreasing size and by increasing volumetric concentration. Further, the ratio of nanofluid and base fluid dynamic viscosity increased by decreasing size, and by increasing volumetric concentration of nanofluid.

Jajja *et al.* [18] performed experiment on different integral fin heat sinks by varying spacing with water as a coolant at power of 325 W. They concluded that thermal resistance and base temperature decreased with the increase of flow rate and decrease of fin spacing. They found maximum enhancement ratio of 1.39 in overall heat transfer coefficient against 3.9 in area enhancement ratio.

Recent research shows that the thermal conductivity of nanofluids is inversely proportional to grain size. Keblinski *et al.* [19] explained this by considering particles Brownian motion, liquid layering at liquid/particle interface, heat transport nature and nanoparticles clustering effects. They found that the Brownian motion role was not important as compared to other studied factors in heat transport properties. They also showed that decrease in thermal conductivity occurred with increase of particle diameter.

Naphon and Nakharintr [20] compared cooling rate achieved by TiO_2/H_2O nanofluid with cooling rate achieved by de-ionized water using three different rectangular heat sinks by varying height. They found that heat transfer rate increased and pressure drop decreased with increase of fin height. They observed 11%, 27% and 42.3% enhancement in average heat transfer rate compared to water with 1.0 mm, 1.5 mm and 2.0 mm height heat sinks, respectively.

Shenoy *et al.* [21] performed experiments on multi-walled carbon nanotubes grown as integral part of silicon minichannel with water as a coolant. Two different multi-walled carbon nanotubes minichannel were tested, one minichannel had 6 × 12 (rows, columns) and other was fully covered with multi-walled carbon nanotubes. Experiment showed that 6 × 12 bundle device and fully covered multi walled nanotubes were capable of removing base heat flux 2.3 times and 1.6 times respectively, while keeping same base temperature.

Hung *et al.* [22] computationally investigated hydraulic and thermal performance of three dimensional porous microchannel having rectangular, trapezoidal, outlet enlargement, thin rectangular, sandwich and block distributions for Reynolds number range of 45-1350. They found, porous

configuration of heat sink exhibited better thermal performance and became prominent at high Reynolds number, while pressure drop also increased with addition of porous material.

Yang *et. al.* [23] analyzed air cooling rate on restricted geometries heat sinks. They compared the result of plate, slit and louver fin heat sinks. They found that louver fin heat sink had better heat transfer rate than plate and slit fin heat sinks. However, it also showed more pressure drop. Experimental result showed that best thermal design of louver heat sink was at 1.65 mm fin spacing, which reduced 25% requisite heat dissipation area.

Above literature study shows that most of the researcher focused on heat sink geometry in order to maintain temperature in a safe threshold range. The aim of the present study is to minimize the manufacturing cost and complexity involved in manufacturing of minichannel/microchannel heat sinks. In this investigation a simple flat heat sink is used; Alumina and copper based nanofluids with 0.251% and 0.11% volumetric concentration were tested at different Reynolds number.

Experimental setup

The pictorial and schematic view of test rig is shown in Fig. 1a and 1b respectively. The rig was consisted of fluid reservoir, two brushless DC pumps (DC30A-1230, China), radiator (R121225BH, Gigabyte, Taiwan), needle valve, micro flow meter (FTB333D, Omega, USA), heat sink, copper block, two surface heater, K type thermocouples (5TC-TT-KI-30-1M, Omega, USA), data acquisition system (34972A, Agilent, USA) and DC power supply (8102, Lodestar).

One litter of fluid from liquid reservoir was pumped by two DC brushless pumps, connected in parallel to each other, to maintain the constant flow rate. Each pump consumed 4W with a maximum flow rate of 4 LPM. Pumps were able to manage pressure drop produced by experimental loop.

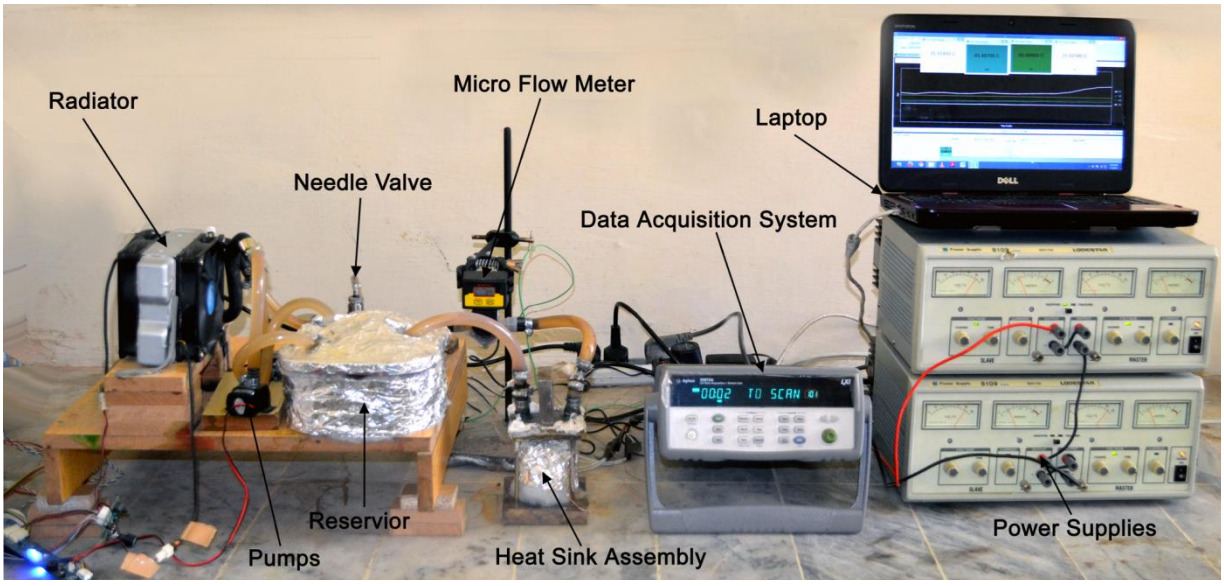

Fig. 1a. Experimental setup

The energy absorbed by fluid from heat sink was dissipated by radiator, which maintained the fluid temperature of 38 °C at the inlet of heat sink. The radiator of a commercial CPU liquid cooling system (GALAXY) was used. Next to the radiator, needle valve and micro flow meter was installed to control and measure the required flow rate respectively. The full scale accuracy of flow meter was ±7%.

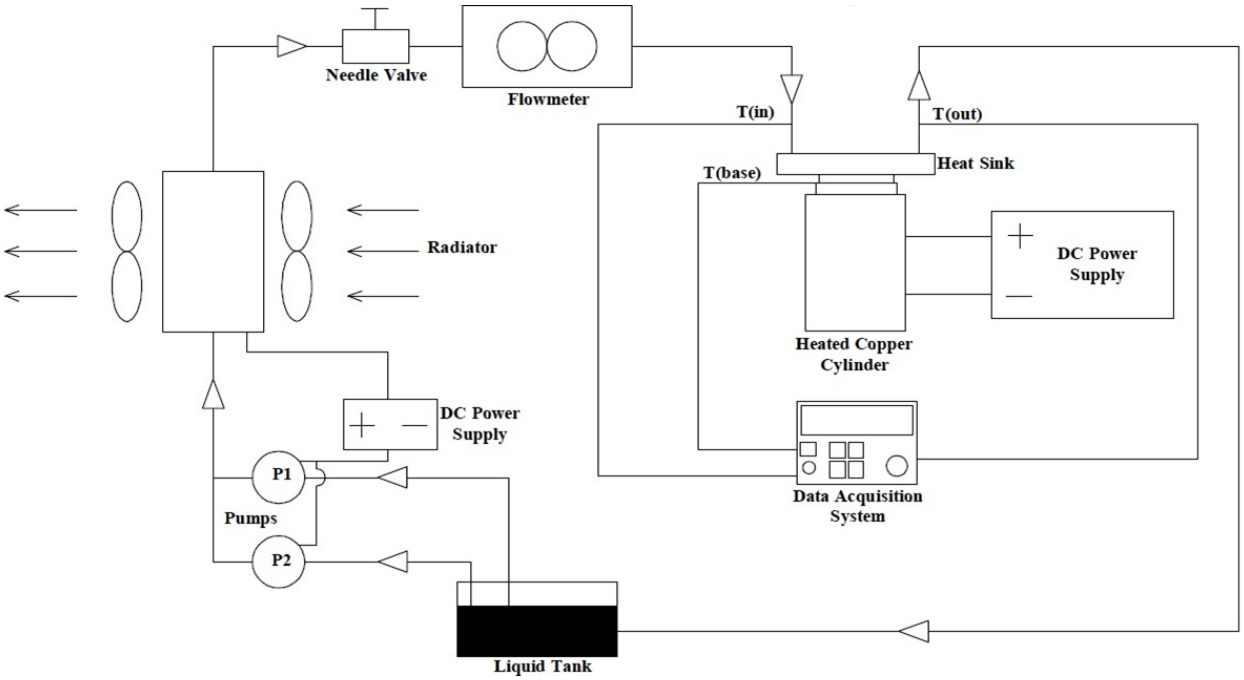

Fig. 1b. Schematic diagram of experimental setup

The heat sink was manufactured by CNC machine. The specification of heat sink is shown in Tab. 1 (see Fig. 2a). At the center of the base, there was a hole of 1 mm with depth of 2.5 mm, which was 1mm below the upper surface of heat sink as show in Fig. 2b. One thermocouple was inserted in the hole to measure the base temperature of heat sink. The protruded base of heat sink was mounted on the heating block.

The heating block was mainly consisted of copper circular cylinder. A slot of 1 mm × 1 mm along the radius was made on the top of the cylinder to insert a thermocouple to the base of heat sink as shown in Fig. 2c.

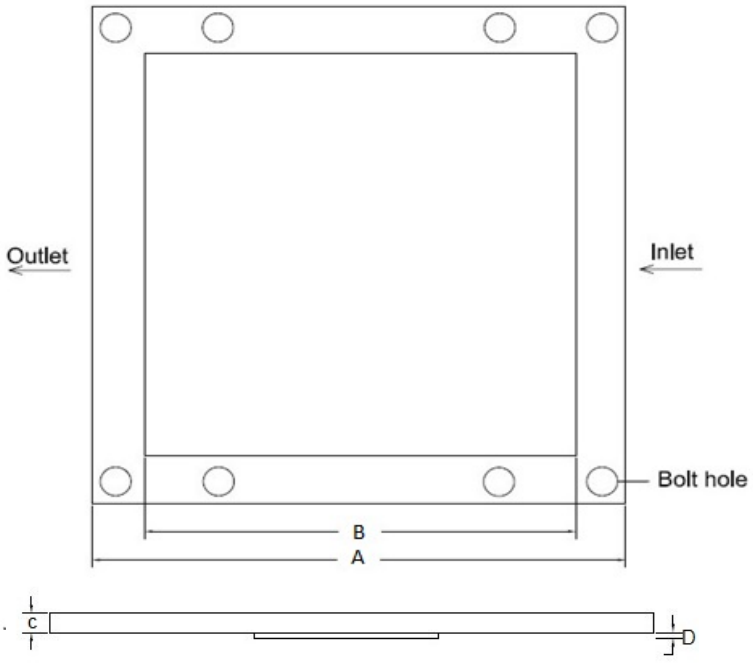

Fig. 2a. Drawing of heat sink

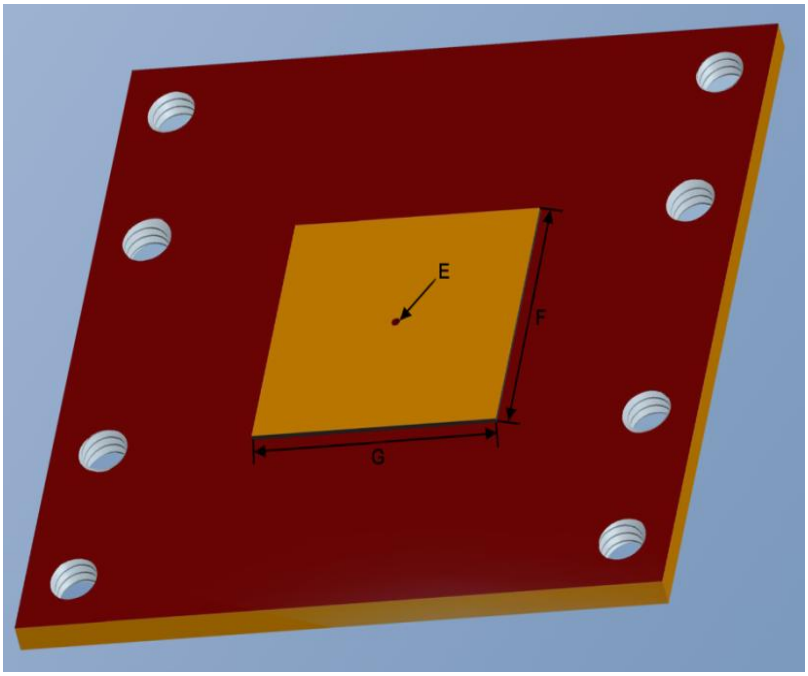

Fig. 2b. Base of heat sink

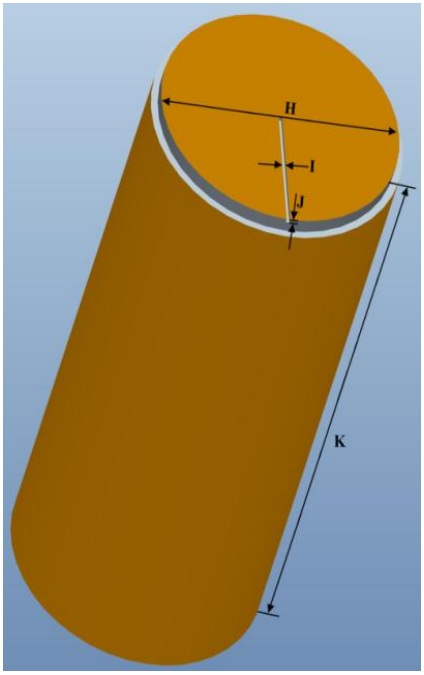

Fig. 2c. Copper cylinder

Two surface heaters, each of 386 Ω resistance, were mounted parallel on the copper cylinder. Two DC power supplies connected in series were responsible to generate 260 W through the heaters. The voltage and current was set to 224 V and 1.16 A respectively. To minimize thermal resistance between copper cylinder and heat sink, high heat conductive silver thermal paste was used. Before application of thermal paste, surface of both of heat sink base and copper cylinder upper surface was finished by 1500 micron fine sand paper. Four nuts and bolts arrangement was used for fit assembling of heat sink with copper cylinder as shown in Fig.3.

To measure the inlet, outlet, base and ambient temperature, Agilent data acquisition system was used. The employed nanofluid, alumina and copper were prepared at National Center of Physics (NCP), Pakistan. These fluids were water based and stable for one month at ambient temperature. The concentration of each nanofluid was 1% wt.

Table 1. Specifications of heat sink geometry (mm)

No.	Geometry	Dimensions
1.	Heat sink	Total length (A) = 76 Characteristic length (B) = 60 Thickness (C) = 3 Extruded part thickness (D) = 0.5 Hole diameter (E) = 1 Extruded part area (F×G) = 28.7×28.7
2.	Copper cylinder	Diameter (H) = 28 Slot width (I) = 1 Slot height (J) = 1 Cylinder height (K) = 80

Data reduction

When fluid passes from heat sink, it extracts heat. The heat transfer rate between the heat sink and the liquid is calculated by following Eq. (1),

$$Q = \dot{m}\, c_p\, (T_{out} - T_{in}) \quad (1)$$

Density, specific heat and viscosity are calculated at mean temperature of fluid given by following Eq. (2),

$$T_m = (T_{in} + T_{out})/2 \quad (2)$$

The heat transfer rate in term of overall heat transfer coefficient is calculated by Eq. (3),

$$Q = UA_r(LMTD) \quad (3)$$

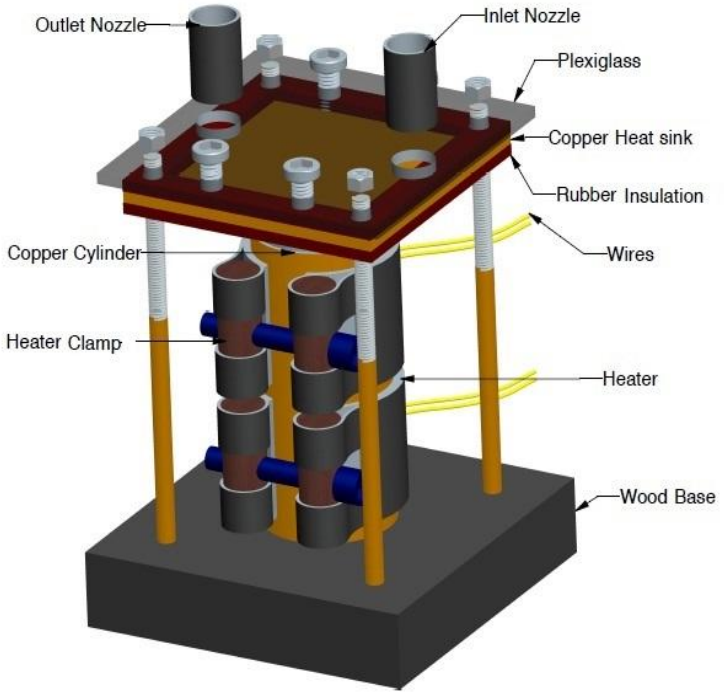

Fig. 3. Heat sink assembly

Where, $A_r = B^2$ (4)

LMTD is log mean temperature difference. This can be calculated by Eq. (5),

$$LMTD = ((T_b - T_{in}) - (T_b - T_{out}))/\ln\left((T_b - T_{in})/(T_b - T_{out})\right) \quad (5)$$

By comparing Eq. (1) and (3), we get Eq. (6) for overall heat transfer coefficient,

$$U = \dot{m}c_p(T_{out} - T_{in})/A_r(LMTD) \quad (6)$$

Thermal resistance is another important evaluating parameter of heat sink performance, defined by Eq. (7),

$$R = LMTD/Q \quad (7)$$

Following Eq. (8) is used to calculate the volumetric percentage (∅) of nanofluids from the given wt% [24],

$$\emptyset = w_{np}\rho_{bf}/\left(\rho_{np}(1 - w_{np}) + w_{np}\rho_{bf}\right) \quad (8)$$

Density of nanofluids depends upon density of base fluid, which is dependent of mean fluid temperature. Following Eq. (9) is used to calculate the density of nanofluids [25],

$$\rho_{nf} = \emptyset\rho_{np} + (1 - \emptyset)\rho_{bf} \quad (9)$$

Specific heat capacity of nanofluids is also dependent on base fluid density and specific heat capacity. Following Eq. (10) is used to calculate the specific heat capacity of nanofluids [26],

$$C_{nf} = (\emptyset\rho_{np}C_{np} + (1 - \emptyset)\rho_{bf}\, C_{bf})/\rho_{nf} \quad (10)$$

To calculate the viscosity of nanofluids, a well-known Batchelor [27] relation is used,

$$\mu_{nf} = \mu_{bf}(1 + 2.5\emptyset + 6.2\emptyset^2) \quad (11)$$

Reynolds number is calculated as,

$$Re = \rho v d_h/\mu \quad (12)$$

Whereas hydraulic diameter can be calculated as,

$$d_h = 4A_c/P \quad (13)$$

Uncertainty analysis

To incorporate the effect of experimental uncertainty of flow rate, inlet and outlet temperature of coolant and heat sink base temperature on the final calculated parameters of interests, Kline and McClintock [28] method was used. The maximum uncertainties in heat transfer rate, overall heat transfer coefficient and Reynolds number were never found greater than 7.90%, 7.92% and 0.9% respectively in any case.

Results and discussion

Comparison of fluid temperature difference with Reynolds number

The test is performed at low Reynolds number range of 400-800 due to the flow available by two DC brushless pumps. Moreover, for specific heat input, inlet and outlet temperature difference gradually decreases by increasing Reynolds number as shown in Fig. 4.

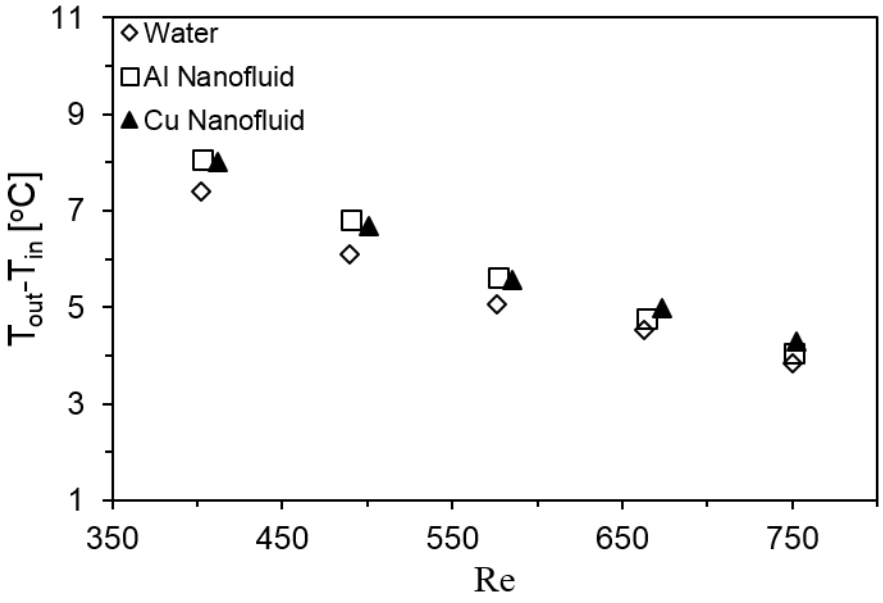

Fig. 4. Comparison of fluid temperature difference with Reynolds number

Comparison of base temperature with Reynolds number

The heat sink's base temperature and the processor's working temperature are analogous to each other. The systematic effects of Al_2O_3/H_2O and Cu/H_2O nanofluids is studied on base temperature of heat sink and compared with water at five different Reynolds number. The base temperature decreases with increase of Reynolds number for all tested fluids as shown in Fig. 5. Moreover, high concentrations of nanoparticles in fluid may lead to high heat transfer rate by that fluid. Although, Al_2O_3 nanoparticles have lower thermal conductivity than copper nanoparticles, but due to high volumetric concentration of alumina nanoparticles, Al_2O_3/H_2O nanofluid shows lower base temperature than that of Cu/H_2O nanofluid at same Reynolds number. However, at high Reynolds number, copper nanofluid shows more base temperature reduction and becomes nearly equal to alumina nanofluid base temperature. Water shows less reduction in base temperature with respect to both Al_2O_3/H_2O and Cu/H_2O nanofluids. As an overall, Al_2O_3/H_2O and Cu/H_2O nanofluids show 5.39% and 3.89% less base temperature compared to water respectively.

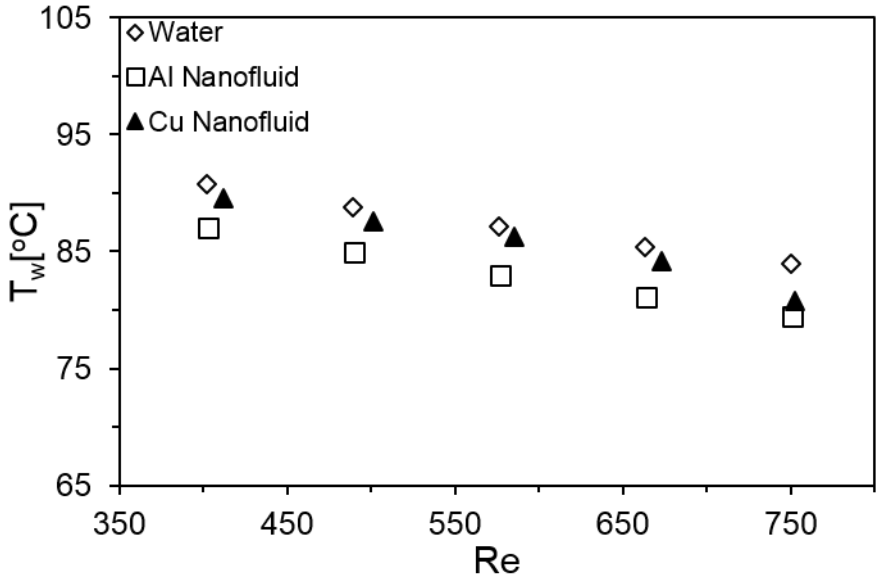

Fig. 5. Comparison of base temperature with Reynolds number

Comparison of heat transfer rate with Reynolds number

Heat transfer rate as a function of Reynolds number is shown in Fig. 6. The trends are different for different kind of fluids. For Al_2O_3/H_2O nanofluid, at low Reynolds number, heat flow rate increases with increase of Reynolds number first. After that reduction in heat rate occurs for further increase of Reynolds number. Al_2O_3/H_2O nanofluid shows maximum enhancement 8.34% compared to water at Reynolds number of 577.

Now consider Cu/H_2O nanofluid and water case, which are following nearly same pattern. Heat transfer rate is not following specific trends for both cases and makes a zigzag graph. At lower Reynolds number range, Al_2O_3/H_2O nanofluid shows better performance as compared to both Cu/H_2O nanofluid and water. However, at higher Reynolds number, Cu/H_2O nanofluid shows better performance even more than Al_2O_3/H_2O nanofluid.

A maximum enhancement of 4.66% with respect to water is found at Reynolds number of 752. Cu/H_2O nanofluid containing lower concentration of nanoparticle is more effective than Al_2O_3/H_2O nanofluid at higher Reynolds number.

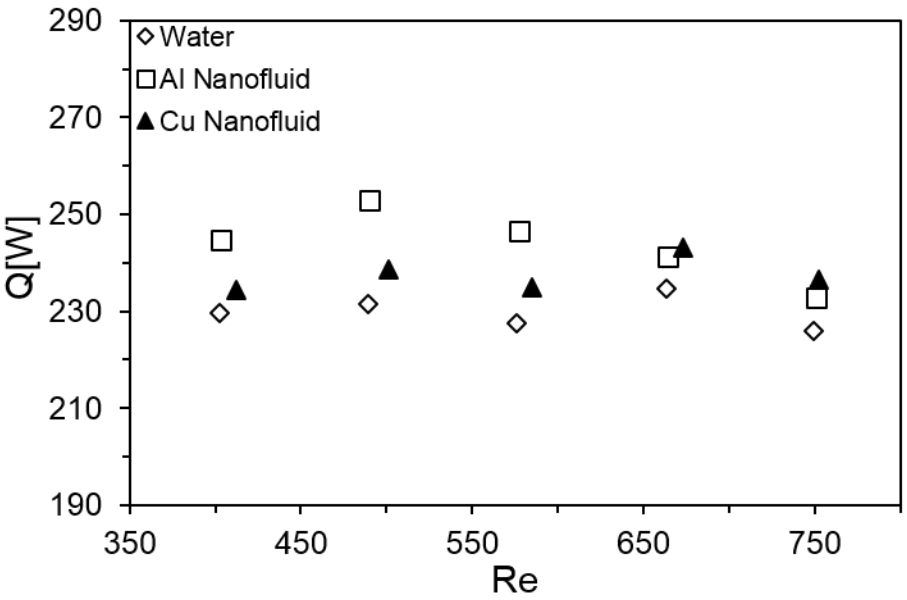

Fig. 6. Comparison of heat transfer rate with Reynolds number

Comparison of overall heat transfer coefficient with Reynolds number

The overall heat transfer coefficient is the best criteria to evaluate heat transfer characteristic because overall heat transfer coefficient includes both base temperature and heat transfer rate. Fig. 7 shows the comparison of Reynolds number and overall heat transfer coefficient for all tested fluids. The overall heat transfer coefficient increases with increase of Reynolds number for all tested fluids. For Al_2O_3/H_2O nanofluid, overall heat transfer coefficient increases gradually with the increase of Reynolds number. Overall heat transfer coefficient increases with a high rate at lower Reynolds number as compared to its enhancement at high Reynolds number. Alumina nanofluid shows a maximum overall heat

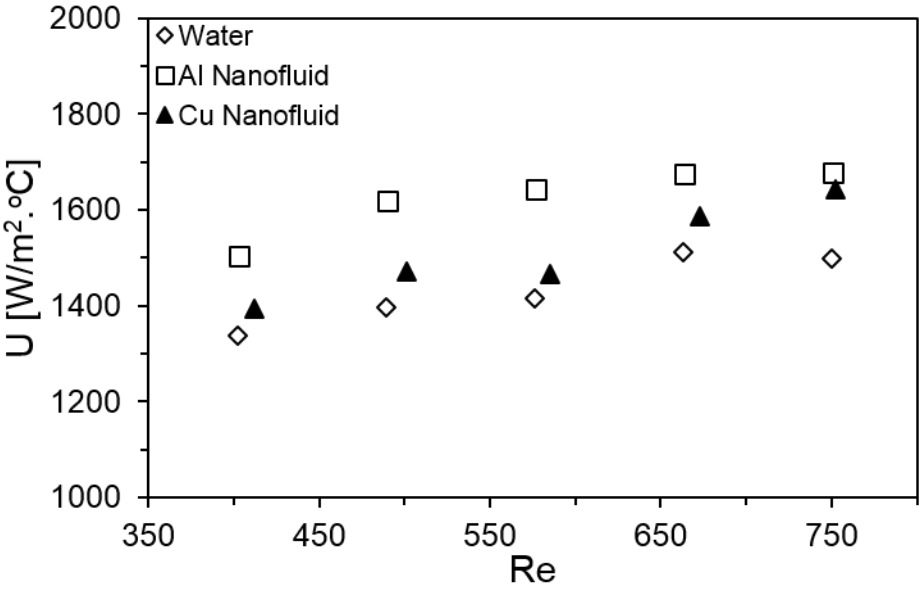

Fig. 7. Comparison of overall heat transfer coefficient with Reynolds number

transfer coefficient value of 1678W/m^2°C. For Cu/H_2O nanofluid, at lower Reynolds number, its performance with respect to Al_2O_3/H_2O nanofluid is less efficient, but with the increase of Reynolds number, its performance improves and becomes almost equal to Alumina nanofluid at 721 Reynolds number. Copper nanofluid shows a maximum overall heat transfer coefficient 1644.46W/m^2°C. Overall, Al_2O_3/H_2O and Cu/H_2O nanofluids show 12.56% and 9.80% enhancement compared to water respectively.

Comparison of thermal resistance with Reynolds number

Figure 8 shows the thermal resistance variation with respect to Reynolds number for all tested fluids. All fluids show nearly similar trend against Reynolds number and thermal resistance decreases with increase of Reynolds number. Al_2O_3/H_2O nanofluid shows the lowest thermal resistance as compared to other two fluids. Alumina nanofluid shows a minimum thermal resistance of 0.17 K/W at Reynolds number of 751. For Cu/H_2O nanofluid, thermal resistance gradually decreases with the increase of Reynolds number. Copper nanofluid shows minimum thermal resistance of 0.17K/W at Reynolds number 752.

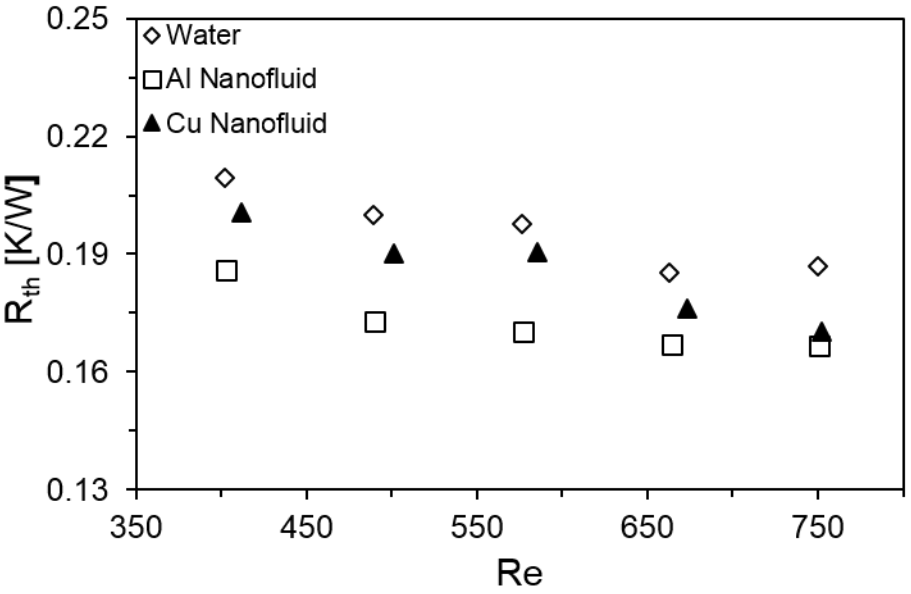

Fig. 8. Comparison of thermal resistance with Reynolds number

Conclusions

Al_2O_3 and Cu nanofluids with 0.251% and 0.11% volumetric concentrations with water as a base fluid were tested using a flat plate heat sink. Following are the important findings obtained from the experiment:

1. Both nanofluids showed higher heat transfer performance in comparison with pure water.
2. Al_2O_3/H_2O nanofluid showed greater heat transfer rate than Cu/H_2O nanofluid at low Reynolds number, but copper behaved more effectively at high Reynolds number.
3. Heat transfer rate was not necessarily increased or decreased with the increase of Reynolds number.

4. The lowest base temperature achieved was 79.45 °C by Aluminium oxide nanofluid at Reynolds number of 751.
5. Al_2O_3/H_2O and Cu/H_2O nanofluids showed 8.34% and 4.66% enhancement in heat transfer rate compared to water respectively.
6. Al_2O_3/H_2O and Cu/H_2O nanofluids exhibited 12.56% and 9.80% augmentation in overall heat transfer coefficient compared to water respectively.

Nomenclature

A_r	heat transfer area of the flat plate heat sink [m^2]
A_c	cross sectional area [m^2]
c_p	specific heat [$kJkg^{-1}°C^{-1}$]
d_h	hydraulic diameter [m]
$\dot{m}$	mass flow rate of fluid circulating through the heat sink [kgs^{-1}]
P	perimeter [m]
Q	heat removed by the fluid circulating through the heat sink [W]
R	thermal resistance of heat sink [KW^{-1}]
T	temperature [°C]
U	overall heat transfer coefficient [Wm^2K^{-1}]
w	weight fraction
$\emptyset$	volumetric fraction
ρ	density [kgm^{-3}]
μ_{bf}	viscosity of base fluid [$kgm^{-1}s^{-1}$]

Subscripts

bf	base fluid
in	inlet
m	mean
nf	nanofluid
np	nanoparticle
out	outlet

Abbreviation

LMTD	log mean temperature difference
LPM	liter per minute
Re	Reynolds number ($= \rho v d_h/\mu$)

References

[1] Tuckerman, D.B., Pease, R.F.W., High-performance heat sinking for VLSI, *IEEE Electron Device Letters EDL 2 (5)* (1981) 126–129.

[2] Schubert, K., et al., Microstructure devices for applications in thermal and chemical process engineering, *Microscale Thermophysical Engineering 5* (2001) 17–39.

[3] Kandlikar, S.G., A roadmap for implementing minichannels in refrigeration and air-conditioning systems current status and future directions, *Heat Transfer Engineering 28–12* (2007) 973–985.

[4] Sobhan, C.B., Peterson, G.P., Microscale and Nanoscale heat transfer fundamentals and engineering applications, CRC Press, Taylor & Francis Group, Boca Raton, Florida, 2008.

[5] Xie, X.L., et al., Numerical study of turbulent heat transfer and pressure drop characteristics in a water cooled minichannel heat sink, *J. Electron. Packag. 129* (2007) 247-255.

[6] Steinke, M.E., Kandlikar, S.G., Review of single phase heat transfer enhancement techniques for application in microchannels, minichannels and microdevices, *Heat and Technology 22–2* (2004) 3.

[7] Pak, B.C., Cho, Y.I., Hydrodynamic and heat transfer study of dispersed fluids with submicron metallic oxide particles, *Exp. Heat Transfer 11 (2)* (1998) 151–170.

[8] Ho, C.J., et al., An experimental investigation of forced convective cooling performance of a microchannel heat sink with Al_2O_3/water nanofluid, *Appl. Therm. Eng. 30 (2–3)* (2010) 96–103.

[9] Lee S., et al., Measuring thermal conductivity of fluids containing oxide nanoparticles, *J. Heat Transfer 121 (2)* (1999) 280–290.

[10] Lee, J., Mudawar, I., Assessment of the effectiveness of nanofluids for single phase and two phase heat transfer in microchannels, *Int. J. Heat Mass Transfer 50 (3–4)* (2007) 452–463.

[11] Sohel, M.R., et al., An experimental investigation of heat transfer enhancement of a minichannel heat sink using Al_2O_3–H_2O nanofluid, *International Journal of Heat and Mass Transfer 74* (2014) 164–172.

[12] Ho. C. J., et al., An experimental investigation of forced convective cooling performance of a microchannel heat sink with Al_2O_3/water nanofluid, *Applied Thermal Engineering 30* (2010) 96–103.

[13] Anoop, K., et al., Experimental study of forced convective heat transfer of nanofluids in a microchannel, *International Communications in Heat and Mass Transfer 39* (2012) 1325–1330.

[14] Rafati, M., et al., Applications of nanofluids in computer cooling systems (heat transfer performance of nanofluids), *Appl. Therm. Eng. 45-46* (2012) 9-14.

[15] Dixit, T., Ghosh, I., Low Reynolds number thermo-hydraulic characterization of offset and diamond minichannel metal heat sinks, *Exp. Therm. Fluid Science 51* (2013) 227–238.

[16] Peyghambarzadeh, S.M., et al., Performance of water based CuO and Al_2O_3 nanofluids in a Cu–Be alloy heat sink with rectangular microchannels, *Ener. Conversion Management 86* (2014) 28–38.

[17] Corcione, M., Empirical correlating equations for predicting the effective thermal conductivity and dynamic viscosity of nanofluids, *Energy Conversion and Management 52* (2011) 789–793.

[18] Jajja, S. A., et al., Water cooled minichannel heat sinks for microprocessor cooling: Effect of fin spacing, *Applied Thermal Engineering 64* (2014) 76-82.

[19] Keblinski, P., et al., Mechanisms of heat flow in suspensions of nano-sized particles (nanofluids), *International Journal of Heat and Mass Transfer 45* (2002) 855-863.

[20] Naphon, P., Nakharintr, L., Heat transfer of nanofluids in the mini-rectangular fin heat sinks, *International Communications in Heat and Mass Transfer 40* (2013) 25–31.

[21] Shenoy S., et al., Minichannels with carbon nanotube structured surfaces for cooling applications, *International Journal of Heat and Mass Transfer 54* (2011) 5379–5385.

[22] Hung, T-C., et al., Thermal performance analysis of porous-microchannel heat sinks with different configuration designs, *International Journal of Heat and Mass Transfer 66* (2013) 235–243.

[23] Yang, K-S., et al., On the heat transfer characteristics of heat sinks: Influence of fin spacing at low Reynolds number region, *International Journal of Heat and Mass Transfer 50* (2007) 2667–2674.

[24] Rea, U., et al., Laminar convective heat transfer and viscous pressure loss of alumina–water and zirconia–water nanofluids. *Int J Heat Mass Transf 52* (2009) 2042–2048.

[25] Pak, B.C., Cho, Y.I., Hydrodynamic and heat transfer study of dispersed fluids with submicron metallic oxide particles, *Exp. Heat Transfer 11* (1998) 151–170.

[26] Pak, B.C., Cho, Y.I., Hydrodynamic and heat transfer study of dispersed fluids with submicron metallic oxide particles, *Exp. Heat Transfer 11* (1998) 151–170.

[27] Batchelor, G.K., Brownian diffusion of particles with hydrodynamic interaction. *J Fluid Mech 74* (1976) (1) 1–29.

[28] Kline, S. J., McClintock, F. A., Describing Uncertainties in Single-Sample Experiments, *Mech. Eng.*, (1953), 3-8.